Journal of Zhejiang University-SCIENCE A (Applied Physics & Engineering)
ISSN 1673-565X (Print); ISSN 1862-1775 (Online)
www.zju.edu.cn/jzus; www.springerlink.com
E-mail: jzus@zju.edu.cn

Influence of Al_2O_3 particles on the friction and wear behaviors of nitrile rubber against 316L stainless steel*

Ming-xue SHEN[†1,2], Jin-peng ZHENG[2], Xiang-kai MENG[1,2], Xiao LI[2], Xu-dong PENG[†‡1,2]

([1]*Engineering Research Center of Process Equipment and Its Remanufacture of Ministry of Education, Zhejiang University of Technology, Hangzhou 310032, China*)

([2]*College of Mechanical Engineering, Zhejiang University of Technology, Hangzhou 310032, China*)

[†]E-mail: shenmx@zjut.edu.cn; xdpeng@zjut.edu.cn

Received July 20, 2014; Revision accepted Nov. 6, 2014; Crosschecked Jan. 23, 2015

Abstract: The friction and wear properties of nitrile rubber (NBR) against 316L stainless steel pairs were investigated by using a sphere-on-disc test device. The influence of Al_2O_3 particle sizes and the normal load on the tribological behaviors of the pairs were primarily evaluated. The damage behaviors of worn surfaces were analyzed using a scanning electric microscopy (SEM) and a surface profilometer. The results show that the friction coefficient decreased because of particles coming into contact pairs, while particles also play an important role in increasing the wear loss of stainless steel with many furrows on the steel ball surface due to the ploughing effect of hard particles. Large-sized particles could accelerate the wear of rubber, and the micro-cutting scratches of the stainless steel induced by the Al_2O_3 particles embedded in the rubber matrix. However, as the particle's size decreased, the wear loss of the rubber was gradually mitigated. It is obvious that the normal load affected the wear of the rubber to a larger extent than the stainless steel. Moreover, with large particles, the wear loss of rubber increased sharply with increasing the normal load. In addition, the NBR/stainless steel tribo-pairs presented different wear mechanisms, under different conditions, such as having no particles or varied particle sizes.

Key words: Nitrile rubber (NBR), Friction and wear, Al_2O_3 particles, Elastomer seal, Tribological properties
doi:10.1631/jzus.A1400217 **Document code:** A **CLC number:** TH117.1; TQ33

1 Introduction

Nitrile rubber (NBR) has a wide range of applications, such as being used for seals, footwear, mats, and tires, because of its excellent resistance to oils, fuels, and greases. It exhibits specific viscoelastic properties and has good abrasion resistance over a wide temperature range (Yasin *et al.*, 2003; Degrange *et al.*, 2005). As the most common pairs in seal components (e.g., radial lip seals of shafts, valve shaft (rod) seals, and reciprocating piston and piston rod seals), rubber/metal tribo-pairs are widely used in compressors, plunger pumps, hydraulic or pneumatic cylinders in petrochemical equipment, transportation, and construction machinery. Such application conditions require specific material properties either in terms of thermo-mechanical or tribological behaviors. Moreover, the wear behaviors of the rubber play an important role on seal properties, which directly determines the service life of the whole machine (Lee *et al.*, 2012). Usually, elastomers are regarded as prone to wear, the rubber parts are regarded as the main wearing parts and the wear of soft elastomer against hard metal is neglected. While hard particles can

‡ Corresponding author

* Project supported by the National Natural Science Foundation of China (No. 51305398), the National Basic Research Program (973 Program) of China (No. 2014CB046404), and the Zhejiang Provincial Natural Science Foundation of China (No. LQ13E050013)

ORCID: Ming-xue SHEN, http://orcid.org/0000-0002-4224-0067; Xu-dong PENG, http://orcid.org/0000-0002-3502-7946

accelerate the degradation of the elastomer, such as impurities in lubricating oil/grease, wear debris, or pieces of fallen coating material, which come into the interface of the contact pairs in the working process. Previous study has clearly pointed out that rubber and plastic seals in a nuclear main pump can cause severe surface damage to the metal as a counterpart induced by fretting (Darling, 1993). The failure mechanism of the lip seal in a tunnel boring machine was analyzed. The results showed that hard particles such as SiO_2 could be embedded into the tribo-pairs and accelerate the wear of the cobalt-based satellite alloy (Sebastiani *et al.*, 2012).

Recently, the friction and wear properties of rubber have been widely studied. However, most previous studies have mainly focused on the influence of composites, surface modification, aging, and the lubricating medium on the tribological properties of rubber and the tribological behaviors of rubber in a liquid medium with solid particles (Zhang, 1998; Felhös and Karger-Kocsis, 2008; Guan and Wang, 2012; Ren *et al.*, 2013). Although the rapid wear of metal against polymers was observed in the 1960s, the influence of hard particles on the damage behaviors of contact pairs as well as its wear mechanism has remained unclear, especially for rubber and plastic seals (Vinogradov *et al.*, 1965; Dasari *et al.*, 2009). In addition, the tribological behavior of elastomers is greatly influenced by abrasives, including their shape, size, and particles properties, unlike metals or ceramics (Moon *et al.*, 2011; Busse *et al.*, 2011). Therefore, to optimize the design of seals to prolong their service life, the effect of hard particles on the tribological properties of soft rubber against the hard counterpart for rubber/metal must be clearly understood.

In this paper, the friction and wear behaviors of NBR against 316L stainless steel are studied under several different conditions (with and without Al_2O_3 abrasives of different particle sizes). The tribological behaviors and wear mechanism were analyzed in detail. The motivation behind this work is to understand the effect of hard particles, such as abrasives, on the tribological behavior of rubber/steel pairs and to provide a fundamental basis for extending the life of elastomer sealants, which will be helpful in designing sealants for industrial applications.

2 Experimental

2.1 Test device

Fig. 1 shows the schematic illustration of the modified tribological tester with a sphere-on-disc contact. The upper specimen was subjected to a constant normal load F_n; the lower specimen was fixed on a rotating disc. Abrasives were fed onto the tribo-pairs from a hopper via a slotted drum mechanism. The abrasive feed located in front of the tribo-pairs and the drum rotation speed were maintained so that the abrasives were fully fed at a constant feed rate of 150 g/min, which guarantees that the tribo-interface will be immerged in solid particles for each test.

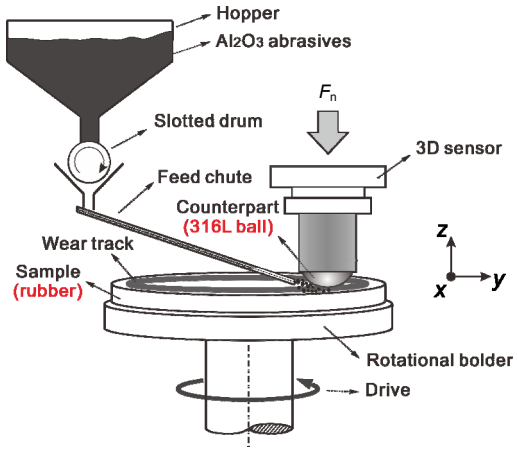

Fig. 1 Schematic illustration of the tribological tester with a sphere-on-disc contact

2.2 Materials and methods

Damage is very common in the rubber-metal contact induced by friction and wear in a liquid seal. Thus, to reveal the damage mechanisms of sealants, tribo-pairs contact with an NBR plate against a 316L stainless steel ball were used in these tests. The main mechanical properties of NBR and 316L stainless steel are shown in Table 1. The rubber is a medium-high percentage of acrylonitrile (35% in weight) material with Mooney viscosity (ML_{1+4} (100 °C)) of 42. Table 2 shows the details of the filler type and content of the NBR in this study. The thickness of the NBR plate was 4 mm, and its surface roughness (R_a) was approximately 0.8 μm. A 316L stainless steel ball with a diameter of 9.5 mm and a surface roughness R_a of 0.04 μm was used as the counter-body. Al_2O_3

Table 1 Main mechanical properties of NBR and 316L stainless steel

Material	Yield strength, σ_s (MPa)	Tensile strength, σ_b (MPa)	Elongation, δ (%)	Elastic modulus, E (GPa)	Density, ρ (g/cm^3)	Hardness
316L	310	580	–	205	7.98	180 HV
NBR	–	16.8	≥450	0.0116	1.32	72 Shore A

particles were used as abrasive particles in the tests. Four different sizes of Al_2O_3 particles with diameters of 200, 110, 60, and 25 μm were selected, each of which had 90% of their particles falling in the range of ±20% based on per particle size analysis. Fig. 2 shows the typical morphology of Al_2O_3 particles, which are highly angular in nature.

In general, the compression ratio of the O-ring is close to 15% for a reciprocating piston and piston rod seals. Therefore, to achieve the equivalent maximum contact stress (about 2, 2.4, and 2.7 MPa, respectively), three different normal loads (F_n=3, 5, and 7 N) were used in this test, which correspond to compression ratios of 13.2%, 16.7%, and 18.5% for the 'O'-type rubber sealing rings. The other main parameters of the test were as follows. The rotating speed of the lower specimen was v=200 r/min (sliding speed of the tribo-pairs v'=4 m/s). All the tests were performed in ambient air (with temperature of (25±2) °C and relative humidity of (60±2)%). The friction force (F_t) was monitored by the 3D sensor throughout the test, which would be interrupted after a set test-time (T=3, 5, 10, 20, 30, and 60 min). First, the NBR plate was cleaned in deionized water separately, and then it was dried by using a drying box for 1.5 h with a constant temperature of 35 °C. In addition, it will be weighed before and after the test. After the test, the worn scars were detected via a scanning electric microscopy (SEM, VEGA3 SBU/SBH, Tescan, Czech Republic) and an energy dispersive spectroscopy (EDX, EDAX–7760/68 ME, Czech Republic). Moreover, the profile of worn scars was determined using a profilometer (XP-2, Ambios Technology, USA).

Table 2 Composition of NBR

Material	Amount (phr)
NBR	100
Sulfur	1.5
Zinc oxide	5.0
Stearic acid	2.0
Carbon black	40
N-cyclohexylbenzothiazole-2-sulphenamide	1.5
Sulfenamide 2,2′-dibenzot	0.5

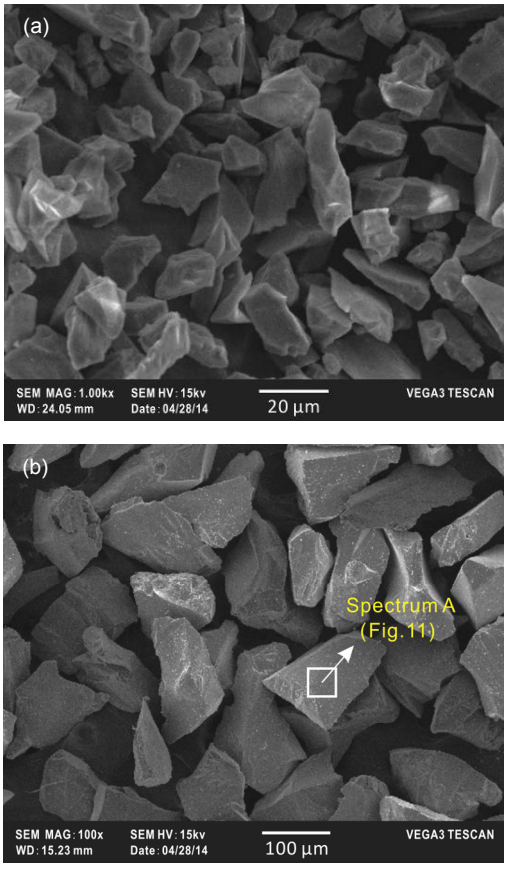

Fig. 2 Typical SEM micrographs of different abrasives
(a) 25 μm Al_2O_3 particles; (b) 110 μm Al_2O_3 particles

3 Results and discussion

3.1 Abrasive size effect

3.1.1 Friction coefficient

The friction coefficients showed significantly different tendencies (Fig. 3), under without particle conditions and with different sizes of the particles. In the initial stage (approximately 4 min), the friction coefficient increased rapidly because of the failure of adsorptive and polluted films on the surface. Under

no particles, the friction coefficient increased slowly and stabilized at approximately 0.75 after a running-in stage. As the particles were 600 μm, the friction coefficient leveled off and was maintained at a value of about 0.56. However, for the other three different size particles (i.e., 200, 110, and 60 μm), the friction coefficients presented a similar trend, which increased quickly to the maximum value (about 0.5), then decreased slowly and finally stabilized approximately at the value of 0.4. However, the fluctuation of the friction coefficient was relatively obvious under larger particle conditions. In summary, the friction coefficient of rubber/metal pairs with Al_2O_3 particles significantly decreased, while the friction coefficient showed two typical evolution features for different sizes of the particles.

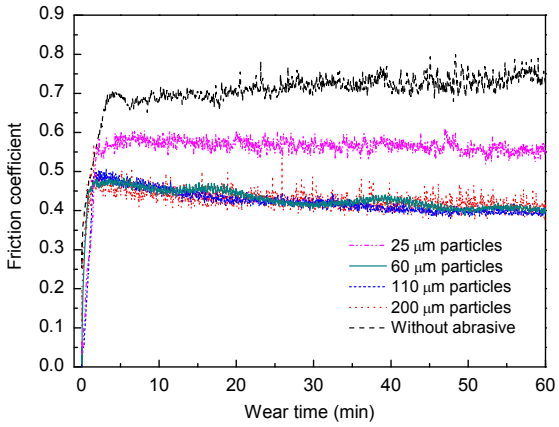

Fig. 3 Variation of friction coefficients with wear time at different particle sizes of the abrasives (F_n=5 N)

3.1.2 Wear loss of NBR

The variation in wear loss of NBR with and without Al_2O_3 particles (F_n=5 N) with different wear time is shown in Fig. 4. Compared with that without Al_2O_3 particles, the size of the Al_2O_3 particles had a great influence on the wear of NBR. Large particles (i.e., 200 and 110 μm) can accelerate the wear of the rubber surface, while small particles (i.e., 60 and 25 μm) can obviously mitigate the wear of rubber. In addition, the wear rate of NBR (wear loss/wear time, rate of slope of the curves in Fig. 4) showed an obvious incremental trend with increasing particle size.

Compared with the no-particles condition, the 2D profile of NBR wear scars (F_n=5 N, T=60 min) also validated that the most serious wear occurred when the NBR contained Al_2O_3 particles with the diameter of 200 μm and the slightest wear occurred when the NBR contained Al_2O_3 particles with the diameter of 60 μm (Fig. 5). In addition, it could be seen that the width of the wear scars was wider under the condition with particles than that under a no-particles condition, because the particles came onto the edges of tribo-pairs and then participated in the wear process.

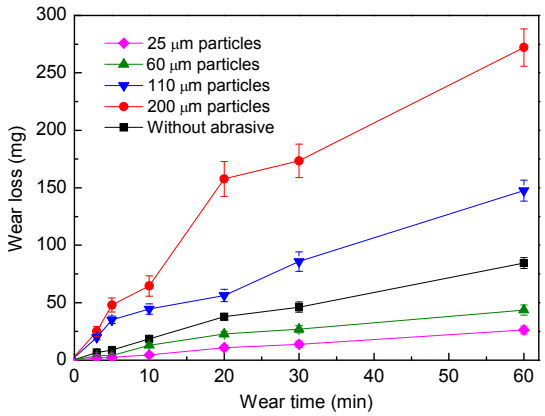

Fig. 4 Variation of wear loss of NBR with wear time for different particle sizes of the abrasives

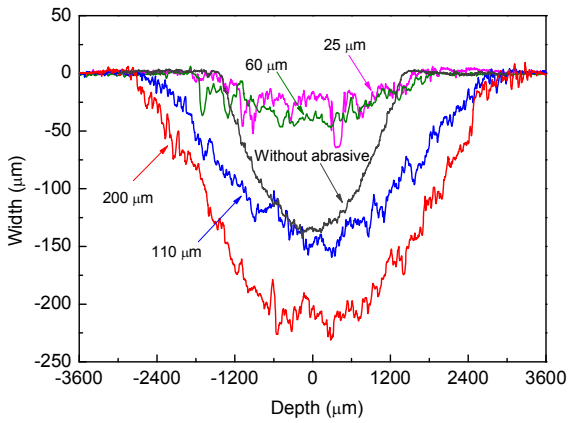

Fig. 5 2D profile of wear scars for NBR containing different abrasives (F_n=5 N, T=60 min)

3.1.3 Damage of the stainless steel ball

The metal counterpart in rubber/metal tribo-pairs may also be seriously worn when hard particles exist. However, few studies have focused on this phenomenon. In this study, the damage of the 316L stainless steel ball was related to the value $K=r/R$, where r and R are the radii of the worn surface and the ball, respectively. Here, the steel ball suffered only minor

damage under the no-particles condition. Thus, the value of K was close to zero and the damage to the ball could be neglected. Fig. 6 shows that the damage behaviors of the steel ball counterpart under various conditions of different particle sizes. For the particles with different sizes, K increased rapidly at first, and then K growth slowed sharply with increasing wear time. For 200 and 110 μm particles, the value of K was close to each other but both were obviously larger than those of the other two types of particles. This trend was similar to that of the effect of Al_2O_3 particles on rubber wear loss shown in Fig. 4.

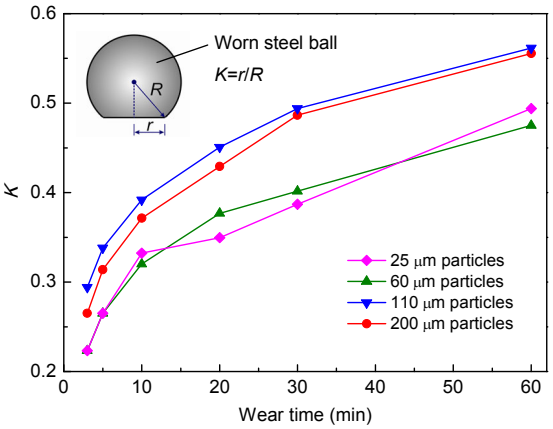

Fig. 6 Variation of K with wear time under various conditons with different particles

3.2 Influence of normal load on wear loss

3.2.1 Wear loss of NBR under different normal loads

To simulate the influence of the seal ring compression ratio on the wear performance of sealants under various conditions with particles, the wear tests of rubber/metal tribo-pairs were conducted under different contact pressures. Fig. 7 shows the wear rate of NBR not containing particles and containing particles with different sizes under different normal loads, after 60 min. The wear loss of rubber increased with increasing the normal load. Moreover, the normal load had an obvious influence on the wear loss of NBR under no particles and with 200 and 110 μm particles. However, for the other two particle sizes (60 and 25 μm), the influence of the normal load on the wear loss of rubber was small, and the wear was relatively slight. Therefore, small size particles can mitigate the wear of rubber. However, when large particles (i.e., ≥60 μm) came into the interface of the rubber/metal tribo-pairs, the wear of the rubber is increased.

3.2.2 Wear loss of the steel ball under different loads

Fig. 8 shows the wear ratio K of the metal ball counterpart after 60 min, under varied normal loads with different particle sizes. Compared with the influence of the normal load on the wear loss of rubber, the wear loss of the steel ball only increased slightly with increasing the normal load, and the influence of particle sizes on the wear loss of the steel ball was not obvious. In addition, the wear ratio K was larger than 0.3 at different particle sizes, but scarcely any wear damage was observed under no particle conditions. Thus, for rubber/metal tribo-pairs, the damage of the metal counterpart was not sensitive to particle sizes. However, severe damage on the counter-metal-surface would occur even if small hard particles came into the seal interface.

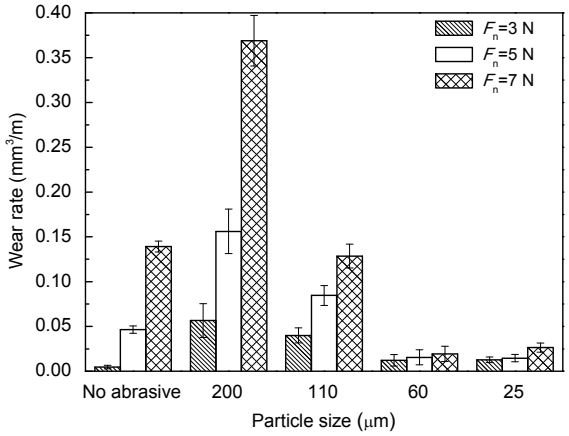

Fig. 7 Wear rate of rubber at different normal loads and particle sizes (T=60 min)

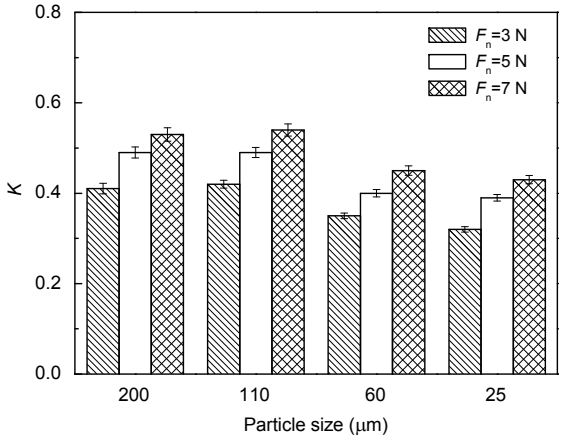

Fig. 8 Wear loss of stainless steel under the conditions of different normal loads and particle sizes (T=60 min)

3.3 Analysis of the wear mechanism

Under the no-particles condition, a series of serrate ridges are generated which are parallel to each other and perpendicular to the sliding direction, and a typical Schallamach wavy pattern (also termed 'waves of detachment' or 'tongue-like' patterns) can be observed on the wear scars (Schallamach, 1958; Zhang, 2004). The formation of the wavy pattern is due to a complex compression/extension strain cycle in the contact area, and this phenomenon is unique to rubber wear (Gatos *et al.*, 2007; Felhös and Karger-Kocsis, 2008; Karger-Kocsis *et al.*, 2008). It is well resolved in the SEM pictures when the wavy pattern is in the direction perpendicular to the sliding direction and then becomes less pronounced towards the flanks of the wear track (Fig. 9a). Moreover, some curled debris can be found on the worn surface (Fig. 9a). Therefore, it can be deduced that the local adhesions were present between the rubber and the metal, and then the adhesive rubber was lengthened repeatedly, in the friction process. Afterwards, a crack might occur when the elongation reaches a critical maximum value, and the detachment of the rubber particles in the form of curled debris appears from the surface layer, when the crack is propagating to meet another. Therefore, the formation of curled debris is the result of adhesive wear and fatigue wear. Moreover, no obvious damage was observed on the steel ball counter-surface (Fig. 9b).

Fig. 10a shows the worn surface morphology of the rubber with 200 μm Al_2O_3 particles. Some granular topography (marked with arrows) and small holes (marked with plus signs) can be observed in Fig. 10a. EDX analyses showed that the aluminum and oxygen content in the granular area was similar to that of the Al_2O_3 particles in Fig. 2, and it was completely different from that of the other worn surfaces of the rubber (Fig. 11). Fig. 11 also indicates that the granular topographies are characteristics of Al_2O_3 particles embedded in the rubber substrates. Thus, the

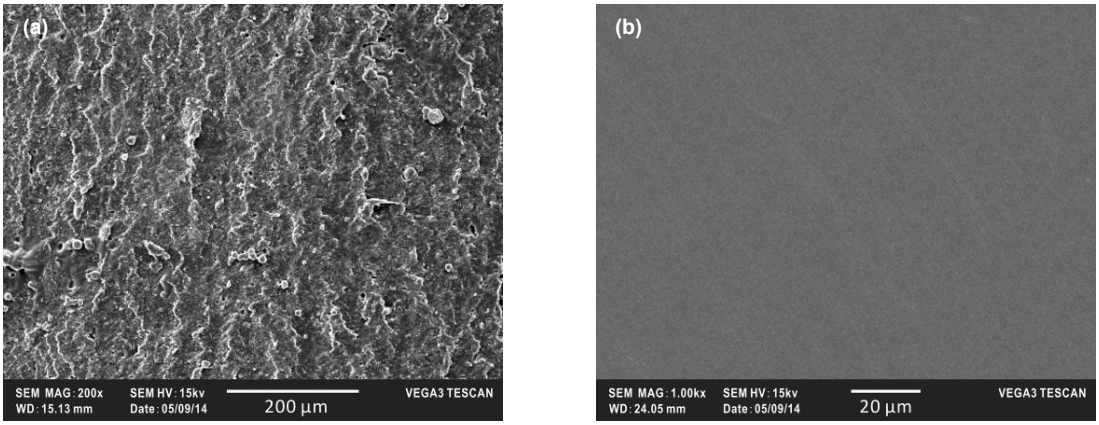

Fig. 9 SEM images of worn surfaces of rubber (a) and steel ball (b) without Al_2O_3 particles

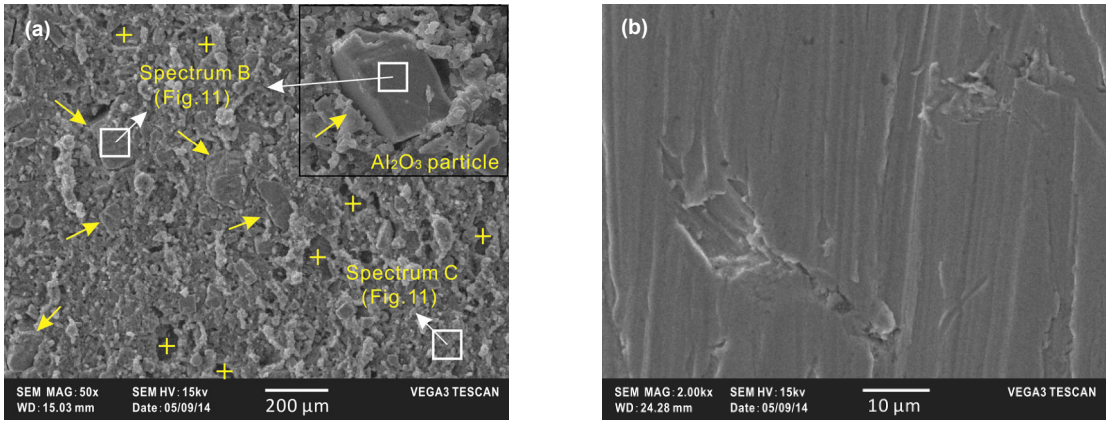

Fig. 10 SEM images of worn surfaces of rubber (a) and steel ball (b) with 200 μm Al_2O_3 particles

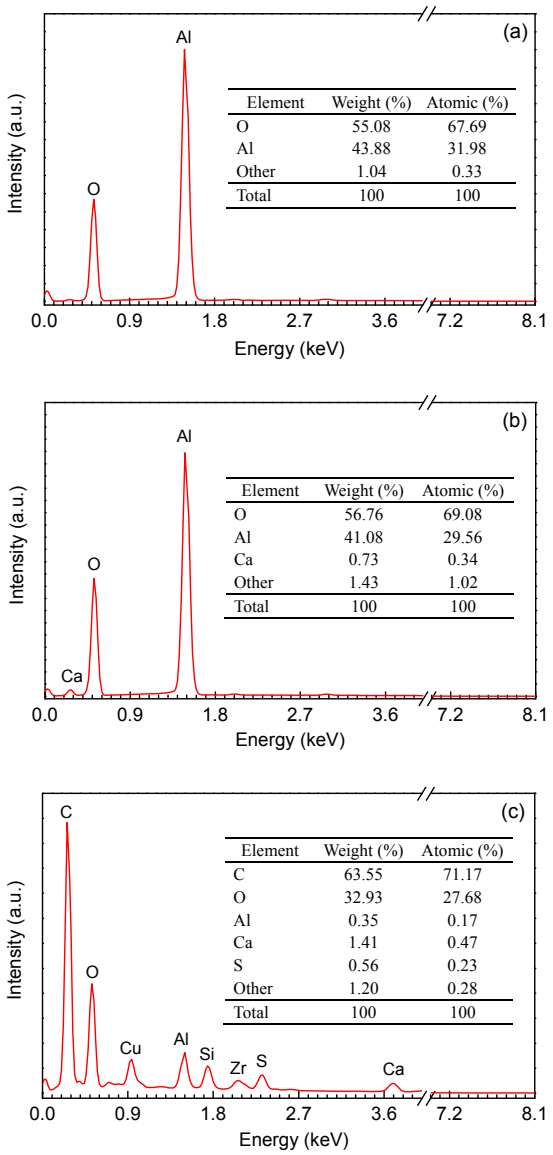

Fig. 11 EDX spectra of the Al_2O_3 particles and the worn surface

(a) Sampled location A (A in Fig. 2b); (b) Sampled location B (B in Fig. 10a); (c) Sampled location C (C in Fig. 10a)

small holes may have been left behind after the shedding of embedded particles in the friction process. The hard particles embedded in rubber would have a 'grinding wheel effect' which caused the rapid wear loss of the metal counterpart, and similar behavior has been reported in other study (Nahvi *et al.*, 2009). Fig. 10b shows the damage morphology of the worn surface of the steel ball. Serious ploughing and micro-cutting pits can be observed in the local regions when NBR with Al_2O_3 particles were used against the steel ball. Therefore, it may be that the main wear mechanisms of the steel ball were the abrasive wear caused by the hard particles as a third-body and the micro-cutting of the hard particle embedded in the rubber.

However, the rubber surface continued to show the damage morphology of pattern wear with small-sized particles (i.e., with 60 μm and 25 μm particles). The serrate ridges were irregularly distributed because of the participation of the particles during the wear process (Fig. 12a). The analysis results of the EDX area scanning also indicated that no embedded Al_2O_3 particles were observed in the rubber. The morphology of the steel ball showed that the shallow furrow parallel to the sliding direction was regularly distributed on the worn surfaces (Fig. 12b). Therefore, the damage morphology of the stainless steel was characterized by ploughing. Accordingly, the main wear mechanism was abrasive wear with the hard particles as a third body.

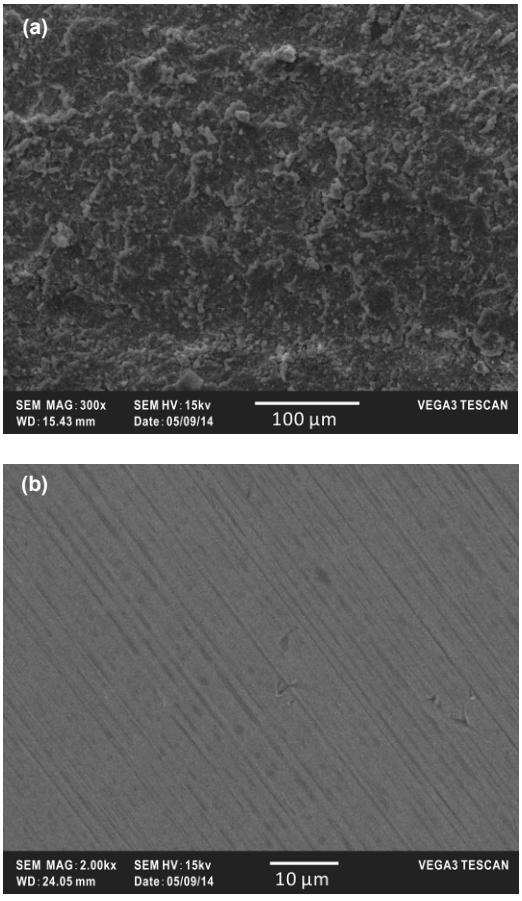

Fig. 12 SEM images of rubber (a) and steel ball (b) worn surfaces with 60 μm Al_2O_3 particle

In addition, the relatively deep grooves near the edges of the worn surface can be observed in the low-magnification of the SEM picture in Fig. 13. However, the wear scar showed two different damage characteristics because of the differences in the local contact pressure. In other words, at the edge of the contact area, the contact pressure was low. As a result, more particles came into the interface, and then the wear mechanism, which was the abrasive wear here, caused more material to be removed. Moreover, the contact pressure in the middle of the contact area was higher than that of the edge. Thus, it was difficult for the particles to enter. Most of the contact area consisted of rubber/metal two-body contact. Thus, irregular pattern wear dominated in the middle of the contact area.

To further understand the influence of Al_2O_3 particles on the friction and wear behaviors of the pairs, Table 3 shows the schematic sketches of the typical wear mechanisms for the tribological behaviors of nitrile rubber against 316L stainless steel with and without Al_2O_3 particles. For the no-particles condition, local adhesion wear occurred between rubber/metal pairs and the adhesive serrate ridges which were regularly distributed along the sliding direction (Table 3). Thus, the wear morphology of rubber was mainly the typical wavy pattern induced by both adhesive wear and fatigue wear. It has been pointed out that the primary ridges of the pattern propagate the formation of wavy shapes with small spacing to secondary ridges with large spacing, as described by Zhang (2004). Therefore, the number of ridges in the contact area gradually increased with increasing wear time. As a result, the friction coefficient also gradually increased (Fig. 2).

For conditions with particles, the particles entered the contact area and acted as the third body layer between the contact pairs (Table 3), reducing the friction coefficient which is due to less local adhesion between the rubber surface and steel ball in the presence of particles (Fig. 2). However, for the small particles conditions, the ridges could not be removed by the scratch of the abrasive wear, but the small particles could separate the local adhesion area between the rubber and metal, and then transfer the two-body wear between the rubber and metal to three-body wear among the particles, rubber, and metal (Molnar *et al.*, 2014) (Table 3). Moreover, the particles greatly mitigated the wear of the rubber due to the particles helping to separate the contact between the rubber and metal, especially for high loads (Fig. 7). As a result, the wear loss of rubber with

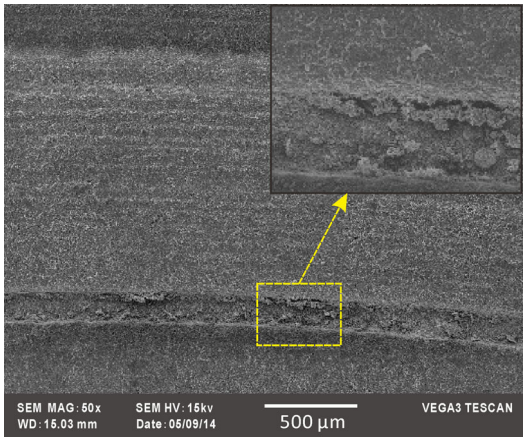

Fig. 13 SEM image of rubber worn surfaces with 60 μm Al_2O_3 particle

Table 3 Schematic sketches of the typical wear mechanisms of nitrile rubber against stainless steel with and without particles*

Condition	Without particles	Large particles	Small particles
Tribo-pairs	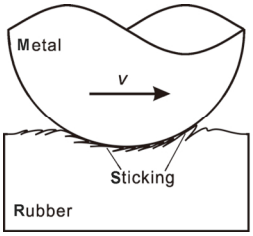	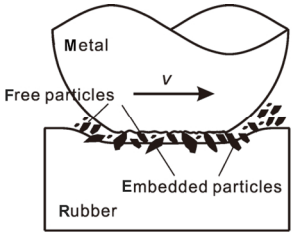	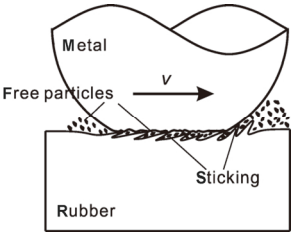
Damage characteristic	Schallamach waves	Ploughing & micro-cutting pits	Slight ploughing & Schallamach waves
Wear mechanism	Adhesive & fatigue wear	Abrasive wear	Abrasive & adhesive wear

* v is a relative velocity between the two tribo-pairs

small particles (i.e., particle sizes of 25 and 60 μm) was less tilted than that without particles, but the contact of hard particles with the metal also aggravated the wear of the steel ball. The friction coefficient between the tribo-pairs was relatively stable (Fig. 2).

However, for large Al_2O_3 particles (i.e., the particles sizes were 200 and 110 μm), the particles could enter the interface, and some particles can be firmly embedded in the rubber substrate. Consequently, two types of abrasives existed between the rubber/metal tribo-pairs, namely, free particles as a third-body and firmly embedded particles (Table 3). During the wear process, the wear in the local parts of the contact area was the three-body wear. Thus, no unique pattern wear can be observed, and the particles also accelerated the wear of rubber. For the metal counterpart, the free particles as a third-body caused the abrasive wear of the metal. Moreover, the embedded particles in the rubber caused a micro-cutting effect on the metal surface. Therefore, coupling the removal mechanisms of the above-mentioned two materials greatly accelerated the wear of the tribo-pairs. Thus, the wear ratio K for the stainless steel ball with large particles was higher than that with small particles (Fig. 6).

Therefore, to avoid the surface wear of rubber/metal tribo-pairs and to extend its operating life, the environment around the rubber/metal tribo-pairs should be kept clean. Moreover, hard particles should be prevented from entering the frictional interface in the engineering process.

4 Conclusions

This work studied the influences of Al_2O_3 particles on the friction and wear behaviors of NBR against 316L stainless steel. The main conclusions can be summarized as follows:

1. Al_2O_3 particles greatly influenced the friction and wear properties of NBR/stainless steel tribo-pairs. The involvement of particles decreased the friction coefficient of rubber/metal tribo-pairs. For rubber, large particles accelerated its wear. When the particle sizes decreased, the particles came into the contact interface and acted as the third-body. As a result, the two-body wear between rubber and metal transferred to three-body wear, which reduced the wear of rubber but aggravated the surface wear of metal under all particle conditions.

2. It was also observed that the damage behaviors of NBR and stainless steel counterpart were different under varied normal loads. Under the large particles and no particles conditions, the wear loss of rubber was remarkably higher than that of small size particles (i.e., particle sizes of 25 and 60 μm) particles when the normal load increased. The influence of normal load on the wear loss of NBR was very small, and the wear was low for NBR with small particles. For the stainless steel counterpart, the wear loss of the steel ball increased very slowly with increasing the normal load.

3. The NBR/stainless steel tribo-pairs presented different wear mechanisms under no particle conditions and with different sizes of the particles. When under no particles condition, a typical wavy pattern can be observed on the wear scars of the rubber, and the damage to the stainless steel was very slight. When particles were involved in the wear process, two-body wear changed to three-body wear, which aggravated the surface wear of the metal. Large particles could be embedded in the rubber; the main wear mechanisms of the steel ball were abrasive wear through hard particles and micro-cutting through the embedded particles in the rubber. However, when the size of the particles was small enough, the wear mechanism of the stainless steel was mainly abrasive wear, whereas the wear mechanism of the rubber is characterized by local wavy pattern wear and abrasive wear.

References

Busse, L., Peter, K., Karl, C.W., 2011. Reducing friction with Al_2O_3/SiO_2-nanoparticles in NBR. *Wear*, **271**(7-8):1066-1071. [doi:10.1016/j.wear.2011.05.017]

Darling, S., 1993. Main coolant pump seal maintenance guide. Technical Report, Electric Power Research Institute, USA.

Dasari, A., Yu, Z.Z., Mai, Y.W., 2009. Fundamental aspects and recent progress on wear/scratch damage in polymer nanocomposites. *Materials Science and Engineering: R: Reports*, **63**(2):31-80. [doi:10.1016/j.mser.2008.10.001]

Degrange, J.M., Thomine, M., Kapsa, P., *et al*., 2005. Influence of viscoelasticity on the tribological behaviour of carbon black filled nitrile rubber (NBR) for lip seal application. *Wear*, **259**(1-6):684-692. [doi:10.1016/j.wear.2005.02.110]

Felhös, D., Karger-Kocsis, J., 2008. Tribological testing of peroxide-cured EPDM rubbers with different carbon black contents under dry sliding conditions against steel. *Tribology International*, **41**(5):404-415. [doi:10.1016/j.triboint.2007.09.005]

Gatos, K.G., Kameo, K., Karger-Kocsis, J., 2007. On the friction and sliding wear of rubber/layered silicate nanocomposites. *Express Polymer Letters*, **1**(1):27-31.

[doi:10.3144/expresspolymlett.2007.6]

Guan, X.Y., Wang, L.P., 2012. The tribological performances of multilayer graphite-like carbon (GLC) coatings sliding against polymers for mechanical seals in water environments. *Tribology Letter*, **47**(1):67-78. [doi:10.1007/s11249-012-9963-2]

Karger-Kocsis, J., Felhos, D., Xu, D., *et al*., 2008. Unlubricated sliding and rolling wear of thermoplastic dynamic vulcanizates (Santoprene®) against steel. *Wear*, **265**(3-4):292-300. [doi:10.1016/j.wear.2007.10.010]

Lee, S.H., Yoo, S.S., Kim, D.E., *et al*., 2012. Accelerated wear test of FKM elastomer for life prediction of seals. *Polymer Testing*, **31**(8):993-1000. [doi:10.1016/j.polymertesting.2012.07.017]

Molnar, W., Varga, M., Braun, P., *et al*., 2014. Correlation of rubber based conveyor belt properties and abrasive wear rates under 2- and 3-body conditions. *Wear*, **320**:1-6. [doi:10.1016/j.wear.2014.08.007]

Moon, S.I., Cho, I.J., Woo, C.S., 2011. Study on determination of durability analysis process and fatigue damage parameter for rubber component. *Journal of Mechanical Science and Technology*, **25**(5):1159-1165. [doi:10.1007/s12206-011-0221-6]

Nahvi, S.M., Shipway, P.H., McCartney, D.G., 2009. Particle motion and modes of wear in the dry sand–rubber wheel abrasion test. *Wear*, **267**(11):2083-2091. [doi:10.1016/j.wear.2009.08.013]

Ren, X.Y., Peng, Z.J., Hu, Y.B., *et al*., 2013. Abrasive wear behavior of TiCN cermets under water-based slurries with different abrasives. *Tribology International*, **66**:35-43. [doi:10.1016/j.triboint.2013.04.002]

Schallamach, A., 1958. Friction and abrasion of rubber. *Wear*, **1**(5):384-417. [doi:10.1016/0043-1648(58)90113-3]

Sebastiani, M., Mangione, V., de Felicis, D., *et al*., 2012. Wear mechanisms and in-service surface modifications of a satellite 6B Co-Cr alloy. *Wear*, **290-291**(30):10-17. [doi:10.1016/j.wear.2012.05.027]

Vinogradov, G.V., Mustafaev, V.A., Podolsky, Y.Y., 1965. A study of heavy metal-to-plastic friction duties and of the wear of hardened steel in the presence of polymers. *Wear*, **8**(5):358-373. [doi:10.1016/0043-1648(65)90167-5]

Yasin, T., Ahmed, S., Makkuchi, K., 2003. Effect of acrylonitrile content on physical properties of electron beam irradiated acrylonitrile-butadiene rubber. *Reactive & Functional Polymers*, **57**(2-3):113-118. [doi:10.1016/j.reactfunctpolym.2003.08.004]

Zhang, S.W., 1998. State-of-the-art of polymer tribology. *Tribology International*, **31**(1-3):49-60. [doi:10.1016/S0301-679X(98)00007-3]

Zhang, S.W., 2004. Tribology of Elastomers. Elsevier, The Netherlands.

中文概要

题　目： Al_2O_3 颗粒对丁腈橡胶/316L 不锈钢配副摩擦磨损行为的影响

目　的： 研究弹性体/金属配副在硬质颗粒环境下的摩擦磨损行为，分析有无颗粒及颗粒尺寸大小对摩擦学特性的影响，为橡塑密封设计提供参考。

创新点： 基于橡胶 O 型圈常见失效机制，模拟橡胶密封圈在颗粒介入时的摩擦磨损行为，探讨硬质颗粒及其颗粒尺寸对橡胶/金属摩擦配副的影响。

方　法： 1. 采用球/平面接触方式，开展丁腈橡胶/金属（316L）配副在 Al_2O_3 颗粒环境下的摩擦磨损行为，通过考察摩擦系数时变曲线、摩擦副磨损形貌及其损伤机制等特性，揭示 Al_2O_3 颗粒对丁腈橡胶/316L 不锈钢配副摩擦磨损行为的影响。

结　论： 1. Al_2O_3 颗粒进入橡胶/金属摩擦配副明显降低摩擦系数、硬质颗粒的犁削作用，加剧金属偶件的磨损；2. 大尺寸的 Al_2O_3 颗粒能嵌入橡胶基体并加速橡胶的磨损，对金属有微切屑作用；然而随着颗粒尺寸的减小，颗粒反而减缓橡胶的磨损；3. 在有无颗粒和不同颗粒尺寸的情况下，橡胶和金属均表现出不同的损伤机制。

关键词： 丁腈橡胶；摩擦磨损；Al_2O_3 颗粒；弹性体密封；摩擦学性能